Permeability and Interaction of Ca^{2+} with cGMP-Gated Ion Channels Differ in Retinal Rod and Cone Photoreceptors

Arturo Picones and Juan I. Korenbrot

Department of Physiology, School of Medicine, University of California at San Francisco, San Francisco, California 94143 USA

ABSTRACT   We studied the ionic permeability of cGMP-dependent currents in membrane patches detached from the outer segment of retinal cone and rod photoreceptors. Reversal potentials measured in membranes exposed to symmetric Na$^+$ but with varying cytoplasmic Ca^{2+} concentrations reveal that the permeability ratio, PCa/PNa, is higher in the cGMP-gated channels of cones (7.6 ± 0.8) than in those of rods (3.1 ± 1.0). Ca^{2+} blocks both channels in a voltage-dependent manner. At any Ca^{2+} concentration, the channel block is maximal near the ionic reversal potential. The maximal block is essentially identical in channels of cones and rods with respect to its extent and voltage and Ca^{2+} dependence. The Ca^{2+} block is relieved by voltage, but the features of this relief differ markedly between rods and cones. Whereas the Boltzmann distribution function describes the relief of block by hyperpolarizing voltages, any given voltage is more effective in relieving the Ca^{2+} block in cones than in rods. Similarly, depolarizing voltages more effectively relieve Ca^{2+} block in cones than in rods. Our results suggest that channels contain two binding sites for Ca^{2+}, one of which is similar in the two receptor types. The second site either interacts more strongly with Ca^{2+} than the first one or it is located differently in the membrane, so as to be less sensitive to membrane voltage. The channels in rods and cones differ in the features of this second site. The difference in Ca^{2+} permeability between the channels is likely to result in light-dependent changes in cytoplasmic Ca^{2+} concentration that are larger and faster in cones than in rods. The functional differences between channels, therefore, may be critically important in explaining the differences in the phototransduction signal of the two photoreceptor types.

INTRODUCTION

In rod and cone photoreceptors light causes closure of cGMP-gated ion channels and thus suppresses the inward current that flows into the cell's outer segment (for review see McNaughton, 1990). In all species studied to date, the photoresponse of cones is faster in time course, less sensitive to light and more robust in its adaptation features than that of rods (for review see Miller et al., 1994). Although the molecular mechanisms underlying these functional differences are not fully understood, it is known that in both cell types cytoplasmic Ca^{2+} in the outer segment regulates the gain, kinetics, and adaptation features of the photoresponse (Torre et al., 1986; Korenbrot and Miller, 1986; Fain and Matthews, 1990; Tomura et al., 1991). We have recently presented evidence that the homeostasis of cytoplasmic Ca^{2+} in the outer segment differs in the two photoreceptor types (Miller and Korenbrot, 1994). This difference may be important in explaining the disparities in phototransduction between cones and rods but cannot be the only explanation (for review see Miller et al., 1994).

In the outer segment, cytoplasmic Ca^{2+} concentration is controlled by the continuous balance between Ca^{2+} entry through the cGMP-gated channels and Ca^{2+} removal by Na/Ca, K exchangers (Yau and Nakatani, 1985; Miller and Korenbrot, 1987). In the dark, influx and efflux are in

balance and the cytoplasmic Ca^{2+} concentration is steady. In the light, the cGMP-gated channels close and Ca^{2+} entry declines. This decline, in the face of sustained activity of the Na/Ca, K exchangers, causes a fall in cytoplasmic Ca^{2+} level. The magnitude and time course of the decrease in Ca^{2+} concentration reflect not only change in fluxes but also the effect of intracellular Ca^{2+}-buffering sites (Ratto et al., 1988; Lagnado et al., 1992; Grey-Keller and Detwiler, 1994). Our recent results (Miller and Korenbrot, 1993a, 1994) suggest that rods and cones differ in every one of the molecular elements that control cytoplasmic Ca^{2+}, i.e., the Ca^{2+} flux through the cGMP-gated channels, the rate of Ca^{2+} clearance by the Na/Ca, K exchanger, and the effectiveness of cytoplasmic Ca^{2+}-buffering sites. In particular, we have hypothesized that the Ca^{2+} permeability of the cGMP-gated channels is higher in cones than in rods (Miller and Korenbrot, 1994).

The cGMP-gated channels in rods and cones are permeable to monovalent and divalent cations but not anions (for review see Yau and Baylor, 1989). The selectivity among monovalent cations in the channels of cones (Picones and Korenbrot, 1992) and rods (Menini, 1990; Furman and Tanaka, 1990) are similar but not identical. Ca^{2+} ions permeate through the channels and also block their conductance in a voltage-dependent manner in rods (Colamartino et al., 1991; Zimmerman and Baylor, 1992; Tanaka and Furman, 1993) and cones (Haynes and Yau, 1990; Picones and Korenbrot, 1992). The channels, however, also differ in some respects. The K_m of cGMP binding is higher in cones (Haynes and Yau, 1990; Picones and Korenbrot, 1992) than in rods (Karpen et al. 1988; Zimmerman and Baylor, 1992), the energy of interaction of cations such as Na$^+$ and Li$^+$

with the channel is different in rods (Menini, 1990; Furman and Tanaka, 1990; Zimmerman and Baylor, 1992) and cones (Picones and Korenbrot, 1992), and the blocking effect of l-cis-diltiazem is also different (Haynes, 1992). Perry and McNaughton (1991) have indirectly demonstrated that the fraction of the current carried by Ca^{2+} through the cGMP-gated ion channels in cones ($\sim$20%) may be twice as large as that in rods ($\sim$10%) (Lagnado et al., 1992; Perry and McNaughton 1991; Nakatani and Yau, 1988; Cobbs and Pugh, 1987). Here we report on direct studies of ion permeabilities in detached outer segment membrane patches aimed at testing the hypothesis that the Ca^{2+} permeability of the channels is higher in cones than in rods. We also contrast some features of the interaction of Ca^{2+} with the ion channels of both receptor types.

MATERIALS AND METHODS

Photoreceptor isolation

We obtained Tiger salamanders (*Ambystoma tigrinum*) from Charles Sullivan (Memphis, TN) and striped bass (*Morone saxitilis*) from Professional Aquaculture Services (Chico, CA). Under infrared illumination we isolated solitary photoreceptors from dark-adapted retinas of either tiger salamanders (rods) or striped bass (single cones) as previously described (Miller and Korenbrot, 1993b, 1994). Solitary photoreceptors were firmly attached to glass coverslips derivatized with concanavalin A (rods) or wheat germ agglutinin (cones). The coverslip formed the bottom of a recording chamber in which cells were maintained under the following solution (in mM): 144 NaCl, 3 KCl, 5 NaHCO$_3$, 1 NaH$_2$PO$_4$, 1 MgCl$_2$, 1 CaCl$_2$, 10 glucose, and 10 HEPES, adjusted with NaOH to pH 7.5, with an osmotic pressure of 305 mOsM.

We compared rods and cones from different species because it was technically convenient, as rods in fish are extremely small and cones in tiger salamander are difficult to isolate. Moreover, we have previously investigated the characteristics of Ca^{2+} homeostasis in intact tiger salamander rods and bass cones (Miller and Korenbrot, 1994). The bathing solutions that best maintain the function of isolated bass cones or tiger salamander rods differ in ionic composition. Because we intended to compare the features of the cGMP-gated channels of the two receptor types under identical physicochemical conditions, we carried out all our measurements in the same ionic solutions. We elected to use solutions that are optimal for fish cones but are $\sim$30% higher in osmotic pressure than those typical for tiger salamander rods. The rods, nonetheless, visually appeared normal and the physiological characteristics of the membrane patches were identical to those we measured in patches detached from cells maintained under optimal solutions.

Under microscopic observation with visible light, we obtained inside-out membrane patches with tight-seal electrodes sealed onto the sides of rod or cone outer segments. The electrodes were made from either aluminosilicate glass (Corning 1724) (1.5 mm outside diameter $\times$ 1.0 mm inside diameter) or borosilicate (Corning 7740) (1.5 mm outside diameter $\times$ 0.85 mm inside diameter) with indistinguishable results. They were filled with (in mM): 157 NaCl, 1 EGTA, 1 EDTA, and 10 HEPES, adjusted with NaOH to pH 7.5, with an osmotic pressure of 305 mOsM. Free Ca^{2+} concentration in this solution was $\leq 10^{-10}$ M and total Na$^+$ concentration was 167 mM. We refer to this as our standard solution.

Ionic solutions

We moved the membrane patches under the water surface from the compartment that held the photoreceptors to a separate compartment containing the same solution we used to fill the electrodes. We delivered test solutions onto the cytoplasmic (outside) surface of the membrane patch through a 100-μm-diameter glass capillary placed within 100 μm of the electrode tip. The solution bathing the cytoplasmic membrane surface was selected from among three possible test conditions, depending on the objective of the experiment: (1) the standard solution, (2) the standard solution with 1 mM cGMP, or (3) the standard solution containing 1 mM cGMP and added CaCl$_2$ in amounts sufficient to yield free Ca^{2+} in the range between 0.01 and 15 mM (calculated with EqCal from BioSoft, Chicago, IL). Total Na$^+$ concentration in the Ca^{2+}-containing solution was 162 mM because additional NaOH was necessary to bring the final pH to 7.5. Therefore, patches exposed to symmetric NaCl solutions between the standard and the Ca^{2+}-containing solutions, in reality, sustained a small gradient of Na$^+$ (167/162, out/in). Because we used a 1 M KCl agar bridge with the bath reference electrode, changes in bathing solutions caused changes in junction potential $\leq$1 mV.

Electrical recordings

We measured membrane currents under voltage clamp at room temperature with a patch-clamp amplifier (Axopatch 200A, Axon Instruments, Foster City, CA). Membrane capacitance was compensated, but not the series resistance. This was of no consequence because we were interested in accurately measuring membrane voltages near zero current conditions. Analog signals were low-pass filtered below 1 kHz with an 8-pole Bessel filter and were digitized on line at 2.5 kHz (FastLab, Indec, Capitola, CA). Membrane voltage was changed with a continuous ramp that swept between -80 and $+80$ mV at a rate of 228 mV/s. To generate I-V curves, the voltage ramp was swept on four successive trials with a 1.2-s interval between trials, and the measured currents were signal averaged over the four trials. We confirmed in selected patches that these I-V curves were identical to those generated from currents elicited by individual voltage steps (Picones and Korenbrot, 1992). Between voltage ramp trials, membrane voltage was held at 0 mV. As is usual, outward currents are positive and the extracellular membrane surface is defined as ground.

Data analysis

To accurately determine the value of the zero current voltage, the point of origin (zero current, zero voltage) in the I-V coordinate plane must be known with certainty. In studies of detached outer segment patches, two sources of error make the determination of the origin point in the I-V plot uncertain. First, in the complete absence of cGMP, the cGMP-gated channels have a low but finite probability of opening (Picones and Korenbrot, 1995a,b). As a consequence, even in the absence of ligand, outer segment patches of both rods and cones exposed to asymmetric solutions of permeable ions exhibit a finite membrane voltage at zero current. Second, the DC offset between the bath electrode and the chloride Ag wire across the seal resistance of the patch electrode may not be fully corrected. To establish with confidence the origin of the I-V plot, we began each experiment by measuring I-V curves under symmetric NaCl solutions, first in the absence and then the presence of 1 mM cGMP. By definition, these two curves cross at precisely the zero voltage, zero current point in the I-V coordinate plane of the cGMP-dependent current. We then exposed the patch to various test solutions in the presence of 1 mM cGMP and ultimately returned to the conditions of symmetric NaCl without cGMP. We analyzed only data collected from patches in which currents measured in the standard solution without cGMP before and after the tests differed by no more than 10%. Statistical errors throughout the text are given as standard deviation. Optimized fits of functions to experimental data were obtained with computer-aided nonlinear, least squares algorithms (Nfit, Galveston, TX). These results were previously presented in abstract form (Picones and Korenbrot, 1995a,)

Results

Fig. 1 illustrates I-V curves measured in detached membrane patches from cone and rod outer segments in the presence of

1 mM cGMP. At this concentration the probability of opening of the cGMP-gated channel is at its maximum in both cones (Haynes and Yau, 1990; Picones and Korenbrot, 1992) and rods (Karpen et al., 1988; Zimmerman and and Baylor, 1992). Under symmetric solutions of NaCl and in the complete absence of divalent ions, the cGMP-dependent currents reversed direction at 0 mV. The I-V curve of cones was essentially linear, but that of rods exhibited a noticeable outward rectification, as has been noted before (Menini, 1990; Furman and Tanaka, 1990; Zimmerman and Baylor, 1992). The addition of Ca^{2+} in the range between 0.01 and 15 mM to the cytoplasmic surface of the membrane caused qualitatively similar changes in the I-V curves of rods and cones; the reversal potential shifted toward more negative values and the current was blocked in a voltage-dependent manner. Detailed inspection, however, demonstrated that the effects of Ca^{2+} were quantitatively different in the two receptor types.

$$\alpha = \frac{RT}{F}, \tag{3}$$

where R, T, and F have their usual meaning, the concentrations of Na^+ and Ca^{2+} on the cytoplasmic and extracellular surfaces are denoted by the subscripts in and out, respectively, and PCa/PNa is the permeability ratio between the cations.

To quantitate the PCa/PNa ratio, we measured V_{rev} in the same patch in the presence of various Ca^{2+} concentration gradients. At each Ca^{2+} concentration tested, we measured V_{rev} in 6–11 different cone patches and in 13–15 different rod patches. Fig. 2 illustrates the average value of the reversal potential and, as a continuous curve, the expected dependence of the V_{rev} on cytoplasmic Ca^{2+} for a given value of the constant PCa/PNa (Eq. 1). To determine the value of this constant, we averaged the PCa/PNa values computed from V_{rev} measured in each patch, at each Ca^{2+} concentration (Eq. 2) (a total of 27

$$\frac{PCa}{PNa} = \frac{-\left[Na_{in}exp\left(V_{rev}\frac{\ln(10)}{\alpha}\right) + Na_{in}exp\left(V_{rev}\frac{\ln(10)}{\alpha}\right)\left(\frac{V_{rev}}{\alpha}\right) - Na_{out} - Na_{out}exp\left(\frac{V_{rev}}{\alpha}\right)\right]}{\left[4Ca_{in}exp\left(V_{rev}\frac{\ln(10)}{\alpha}\right)exp\left(\frac{V_{rev}}{\alpha}\right) - 4Ca_{out}\right]} \tag{2}$$

The Ca^{2+} to Na^+ permeability ratio (PCa/PNa)

In the lower panels of Fig. 1 we illustrate a magnified view of I-V curves near the zero current value. For both cones and rods, the membrane voltage at zero current (the reversal potential, V_{rev}) shifted to progressively more negative values as the cytoplasmic Ca^{2+} concentration increased. The sign of the shift indicates that the cGMP-gated channels are more permeable to Ca^{2+} than to Na^+. For the same Ca^{2+} concentration, however, the voltage shift in cones was larger than that in rods. The magnitude of the shift demonstrates that Ca^{2+} is more permeable (relative to Na^+) through the channels of cones than through those of rods.

In mixtures of Ca^{2+} and Na^+ and under the constant field assumption, the reversal potential of current flowing through ion channels selectively permeable to both cations is given by (Lewis, 1979)

$$V_{rev} = \alpha \ln \frac{Na_{out} + 4\frac{PCa/PNa}{1 + exp\left(\frac{V_{rev}}{\alpha}\right)}Ca_{out}}{Na_{in} + 4\frac{PCa/PNa}{1 + exp\left(\frac{V_{rev}}{\alpha}\right)}Ca_{in}exp\left(\frac{V_{rev}}{\alpha}\right)}, \tag{1}$$

from which it can be shown that

independent values for cones and 28 for rods). For both rods and cones, there is excellent agreement between the experimental data points and the predictions of Eq. 1. The results indicate that for both cell types PCa/PNa is essentially independent of Ca^{2+} concentration. Most importantly, the data demonstrate that the PCa/PNa in cones has an average value of 7.6 ± 0.8, more than twice the average value of PCa/PNa in rods, 3.1 ± 1.0.

Maximal block of membrane conductance by cytoplasmic Ca^{2+}

The effective voltage across detached membrane patches is the sum of the equilibrium voltage, generated by the concentration gradient of permeable ions, and that imposed by the voltage-clamp amplifier. The same asymmetric solutions of Na^+ and Ca^{2+} generate a different equilibrium voltage across cone or rod membrane patches because of the difference in PCa/PNa. Therefore, to contrast the blocking effects of Ca^{2+} in rods and cones under comparable conditions we analyzed I-V curves in which the voltage axis was plotted in terms of electromotive force, V_{emf}. As is conventional,

$$V_{emf} = V_m - V_{rev}, \tag{4}$$

where V_m is the applied membrane voltage and V_{rev} is measured in the asymmetric ionic solution under study. In

FIGURE 1 I-V curves of cGMP-gated currents in inside-out membrane patches detached from the outer segment of single bass cones (*left panels*) or tiger salamander rods (*right panels*). In the presence of 1 mM cGMP on the cytoplasmic surface, the same patch was exposed to symmetric NaCl solutions in either the absence of Ca^{2+} or with Ca^{2+} present in the cytoplasmic surface at concentrations ranging between 0.01 and 15 mM, as labeled. The absence of Ca^{2+}, labeled as zero, is a solution containing 1 mM each EGTA and EDTA. Free Ca^{2+} in this solution can be calculated to be $\leq 10^{-10}$ M. In the absence of cGMP, the membrane conductance for the patches shown was 126 pS for the cone and 445 pS for the rod. Currents were activated by a continuous voltage ramp between -80 and $+80$ mV. Each curve is the signal average of the current generated in four successive ramps. The lower panels illustrate an expanded view of the same data shown in the upper panels. At the same Ca^{2+} concentration gradient, the potential at zero current (reversal potential, V_{rev}) is more negative in value in cones than in rods. For the patches shown, over all Ca^{2+} concentrations, $PCa/PNa = 9.67$ for the cone and $PCa/PNa = 2.83$ for the rod.
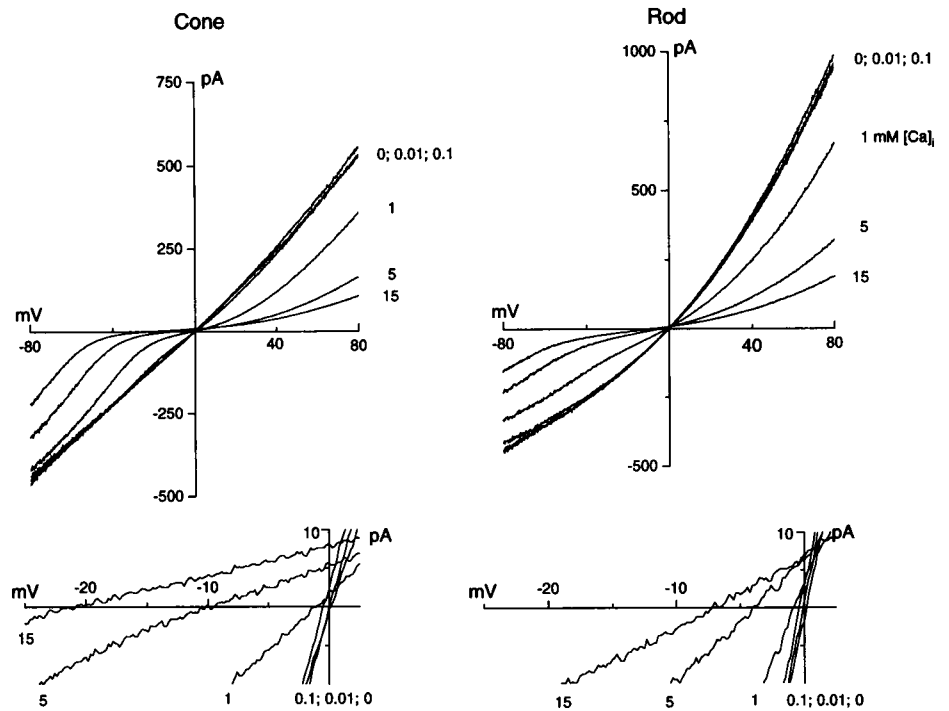
these I-V_{emf} plots, the effects of Ca^{2+} and their voltage dependence can be compared in rods and cones because the voltage axis is now a measure of the net energy difference across the membrane, regardless of the actual value of PCa/PNa.

Fig. 3 illustrates the I-V_{emf} plots of currents measured in cone and rod membrane patches under symmetric NaCl with varying concentration of cytoplasmic Ca^{2+}. In both receptor types, increasing the Ca^{2+} concentration progressively reduced current amplitude at all voltages. The largest membrane conductance block, measured from the slope of the I-V, occurs near the reversal potential. We analyzed the Ca dependence of the maximal conductance block, between 0 and $+20$ mV V_{emf}, in each patch at each of the Ca^{2+} concentrations tested. We then normalized the data by defining the conductance measured in the absence of Ca^{2+} as unity. The maximal conductance was in the range of 1.1 to 7.0 nS in cones and 1.3 to 21.3 nS in rods. Fig. 4 illustrates the average normalized membrane conductance as a function of Ca^{2+} concentration. The points are the average of data from 18 cone patches and 16 rod patches. The maximal block was similar in rods and cones, $\sim 12\%$ of the maximal conductance. The continuous curve in Fig. 4 is an optimal fit to the data points of the Langmuir adsorption isotherm function that describes binding to a single site:

$$\frac{g_m}{g_{max}} = \frac{1}{1 + \dfrac{[Ca]}{K_m}}, \tag{5}$$

where g_m/g_{max} is the normalized membrane conductance, $[Ca]$ is the cytoplasmic Ca^{2+} concentration, and K_m is the binding constant for Ca^{2+} at the blocking site. We fit this function to data from each cone and rod patch. The average value of K_m was 1.12 ± 0.52 mM in cones and 1.37 ± 0.53 mM in rods. These values are not statistically different. That is, channels in rods and cones are similar with respect to the extent of the maximal conductance block caused by cytoplasmic Ca^{2+}, the voltage at which the block occurs, and its Ca^{2+} dependence.

Voltage dependence of conductance block by cytoplasmic Ca^{2+}

Fig. 3 illustrates the fact that, whereas the Ca^{2+}-dependent block is maximal near the equilibrium voltage, in both rods and cones the block decreases for either depolarizing or hyperpolarizing voltages. The effectiveness of voltage in relieving the Ca^{2+} block is different in the two receptor types. To analyze this effect, we replotted the experimental data to measure the normalized membrane conductance, g_m/g_{max}, as a function of the V_{emf}. To this end, we divided the I-V_{emf} curve at each Ca^{2+} concentration tested by the I-V_{emf} curve measured in the same patch but in the absence of Ca^{2+}. Typical g_m/g_{max} versus V_{emf} plots for cones and rods (Fig. 5) demonstrate that hyperpolarizing voltage was more effective in removing the block than depolarizing voltage. However, either hyperpolarizing or depolarizing voltage of the same magnitude was more effective in re-
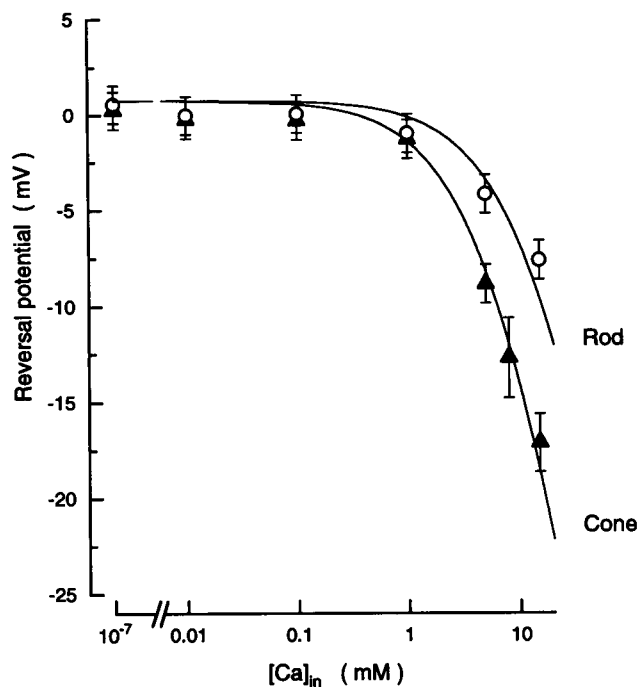
FIGURE 2 Reversal potential measured in 1 mM cGMP in cone (▲) and rod (○) membrane patches exposed to symmetric NaCl solutions in either the absence of Ca^{2+} ($\leq 10^{-10}$ M) or with Ca^{2+} present in the cytoplasmic surface at concentrations ranging between 0.01 and 15 mM. The continuous curve is the expected dependence of reversal potential on cytoplasmic Ca^{2+} (Eq. 1) when the PCa/PNa ratio is 7.6 for cones and 3.1 for rods. In the absence of Ca^{2+}, the reversal potential is not identically zero because the patches sustain a small gradient of Na^+ (167/162 mM, out/in; see Materials and Methods).

lieving the Ca^{2+}-dependent block in cones than in rods. At 15 mM Ca^{2+}, for example, at the extreme of the hyperpolarizing voltage range we explored, −80 mV V_{emf}, the current was blocked by ~60% in rods but only 25% in cones. That is, a fraction of the Ca^{2+}-dependent block could not be relieved by voltage over the range we tested, and this fraction was larger in rods than in cones. Our data in rods at 1 mM Ca^{2+} reproduces those of Colamartino et al.(1991), who previously recognized a voltage-independent component of Ca^{2+} block.

The relief of conductance block by hyperpolarization exhibited a sigmoidal dependence on voltage well described by the Boltzmann distribution function (Fig. 5):

$$\frac{g_m}{g_{max}} = \frac{1}{1 + \exp\left(\dfrac{V_{emf} - V_o}{\kappa}\right)} + A \qquad (6)$$

where V_o is the voltage at which g_m/g_{max} is 0.5 and κ is a sensitivity constant that measures the steepness of the voltage dependence. A is a constant that offsets the minimum value of the normalized conductance away from zero. In Table 1 we present the average values of the adjustable parameters in the Boltzmann equation that best fit the data in five different cone patches and eight rod patches. For hyperpolarizing voltages, the values of V_o and κ were sim-

ilar in both cell types and not statistically different. For depolarizing voltages, only the data from cones was well fit by the function. The data from rods could not be fit by the function. Nonetheless, in the depolarizing range, too, voltage was more effective in relieving the Ca^{2+} block from cones than from rods.

The Boltzmann function describes the distribution of channels between the Ca^{2+}-blocked and unblocked states as a function of the energy provided by V_{emf}. At V_o, half as many channels are blocked as are unblocked. The results shown in Fig. 5 and Table 1 suggest that in both cones and rods a fraction of the Ca^{2+}-blocked channels can be unblocked by essentially the same amount of energy when provided by hyperpolarizing voltages. This energy may be thought of as the binding energy of Ca^{2+} to one site in the channel (site I). However, there is also a second site (site II) for which either Ca^{2+} has a higher energy of interaction or the site is located outside the field of influence of the membrane voltage. In either case, Ca^{2+} cannot be removed from that blocking site even at the highest energy we tested. Cones and rods differ from each other in this second site. In the simplest interpretation, both sites I and II may have comparable energetics in rods and cones, but the effectiveness of the second site as a conductance blocker is different; the site is more effective in blocking the conductance of channels in rods than in those of cones.

DISCUSSION

The cGMP-gated channels in cones and rods share many functional features, but their differences may help explain differences in phototransduction between the receptor types. We have shown here that the Ca^{2+} permeability relative to Na^+ of the channels in cones is higher than that in rods. As previous work has demonstrated that the rate of Ca^{2+} clearance from the outer segment is faster in cones (Perry and McNaughton, 1991; Hestrin and Korenbrot, 1990) than in rods (Hodgkin et al., 1987; Cobbs and Pugh, 1987; Nakatani and Yau, 1988) and, as cytoplasmic Ca^{2+} buffering, although not identical, is similar in the two receptor types (Miller and Korenbrot, 1994), it can be reasonably expected that identical light-dependent changes in outer segment current will cause a greater and faster change in cytoplasmic Ca^{2+} in cones than in rods. Therefore, the various Ca^{2+}-dependent biochemical events now recognized to occur in the outer segment (for review see Miller et al., 1994) will likely be quicker and greater in extent in cones than in rods, helping to explain the differences in their phototransduction signals. However, we do not hold that differences in Ca^{2+} homeostasis are alone sufficient to explain the phototransduction differences. For example, buffering intracellular Ca^{2+} does not trivially convert the response of cones into that of rods or vice versa (Miller et al., 1994).

We propose to generalize to all rods and cones the observations made in but one example of each cell type. We have found the characteristics of the cGMP-gated channels

FIGURE 3 I-V_{emf} curves of currents measured in the presence of 1 mM cGMP in outer segment patches of cones (*left panel*) or rods (*right panel*). The same patch was exposed to symmetric NaCl solutions in either the absence of Ca^{2+} or with Ca^{2+} present in the cytoplasmic surface at concentrations ranging between 0.01 and 15 mM, as labeled. The currents are plotted as a function of the electromotive force, V_{emf}, between -50 and $+50$ mV. Each curve is the signal average of the current generated by four successive ramps. In both rods and cones the maximal current block by Ca^{2+} occurs near the ionic equilibrium voltage, when V_{emf} is near zero. Depolarizing and hyperpolarizing voltages lessen the Ca^{2+} block, but at any given voltage this effect is more effective in cones than in rods.
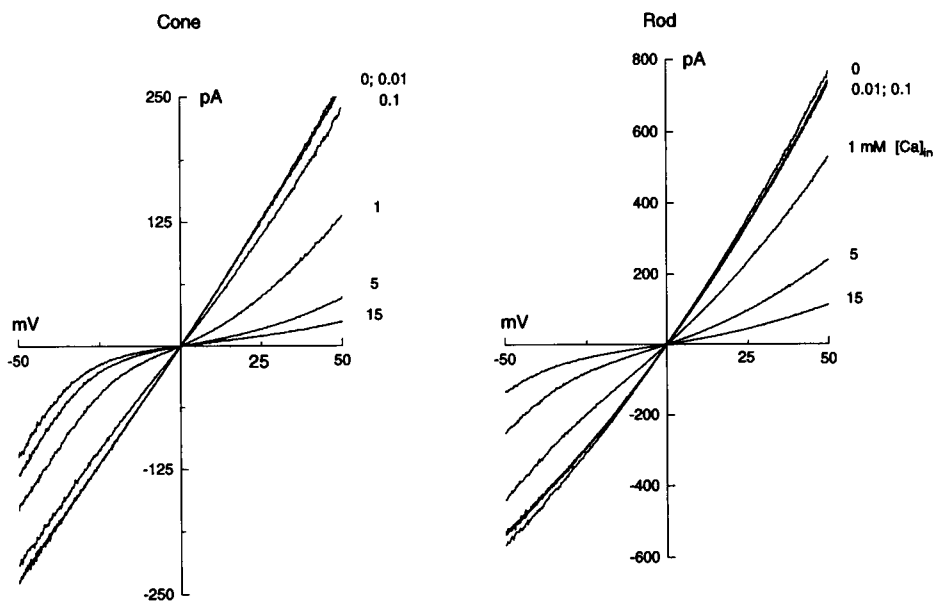
of twin cones in striped bass to be nearly the same as those of single cones reported here. Also, Haynes (1993) in an abstract has reported that the Ca^{2+} permeability of channels in the catfish cone outer segment is high. In frog rods, Tanaka and Furman (1993) have previously measured the

FIGURE 4 Ca^{2+} dependence of the maximal current block in cones (▲) and rods (○). Membrane conductance in the linear region between 0 and $+20$ mV V_{emf} was measured at each Ca^{2+} concentration and normalized by the conductance measured in the absence of Ca^{2+}. The points are the average ± SEM. The continuous curves are Langmuir adsorption isotherms of a single site (Eq. 5) drawn with the average value of K_m measured for cones (1.12 mM) and for rods (1.37 mM). These K_m values are not statistically different.

I-V curve of the cGMP-dependent currents under ionic conditions similar to those we have explored here. Our data are very similar to theirs. Although they did not report a value for PCa/PNa, elsewhere Tanaka (1993) reports a reversal potential from which we calculate a PCa/PNa ratio of 3.6 in the presence of 10 mM Ca^{2+}, a value close to what we report here, 3.1. Zimmerman and Baylor (1992) have previously reported the I-V curves of the cGMP-dependent currents of tiger salamander rod patches measured under gradients of Ca^{2+}. They did not report a specific value for PCa/PNa. Finally, heterologously expressed channels made from recombinant DNA of the α-subunit of bovine rod and cone channels also demonstrate differences in their PCa/PNa ratios (Frings et al. (1995) that are quantitatively similar to the data we report here.

At all Ca^{2+} concentrations tested, in both rods and cones, the maximal block of the cGMP-dependent current occurs near the equilibrium voltage generated by the ion concentration gradient. The maximal block achieved by Ca^{2+} concentrations was approximately the same for both receptor types, $\sim 88\%$. In rods it has been previously shown that, for nonsaturating Ca^{2+} concentrations, the extent of channel block is dependent on cGMP concentration (Colamartino et al., 1991; Tanaka and Furman, 1993; Karpen et al., 1988). We did not explore this feature in cones. At V_{emf} between 0 and $+20$ mV, the Ca^{2+} dependence of the maximal current block in both rods and cones was well described by the adsorption isotherm of a single site. This feature of the Ca^{2+}-dependent block of rod channels was previously described by Zimmerman and Baylor (1992), who found a K_m value at $+30$ mV of 1.4 mM in tiger salamander rods. Tanaka and Furman (1993) have reported qualitatively similar curves in frog rods, but they did not specify a K_m for the site in the same voltage range. Ca^{2+} blockage of the current in cone channels has not been quantitatively analyzed be-
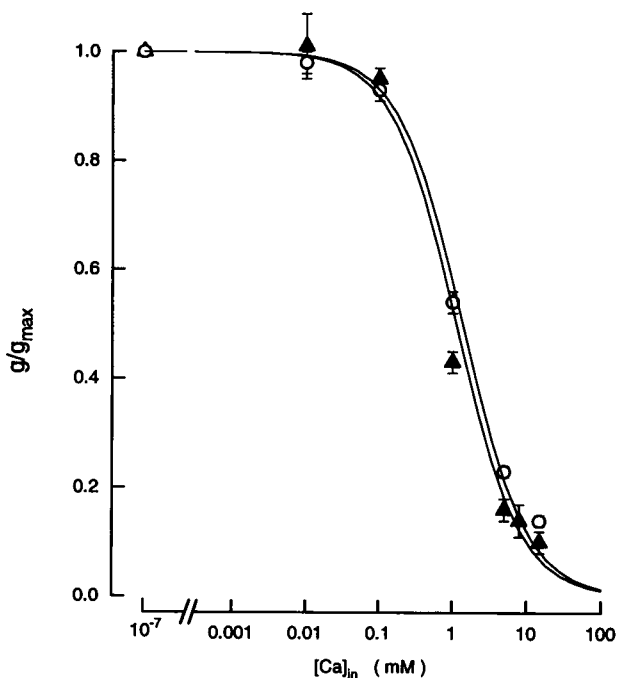
FIGURE 5 Voltage dependence of Ca^{2+} block of cGMP-gated currents in outer segment patches of cones (*left panel*) or rods (*right panel*). We illustrate the normalized conductance, calculated by dividing the *I*-V_{emf} curve at each Ca^{2+} concentration by that measured in the absence of Ca^{2+}, as a function of V_{emf}. The cytoplasmic Ca^{2+} concentration tested is indicated by the label next to each experimental curve. Superimposed on the continuous data line is an optimized fit to the data of the Boltzmann distribution function (Eq. 6) shown by open circles. Table 1 shows the average value of the adjustable constants in the Boltzmann equation.
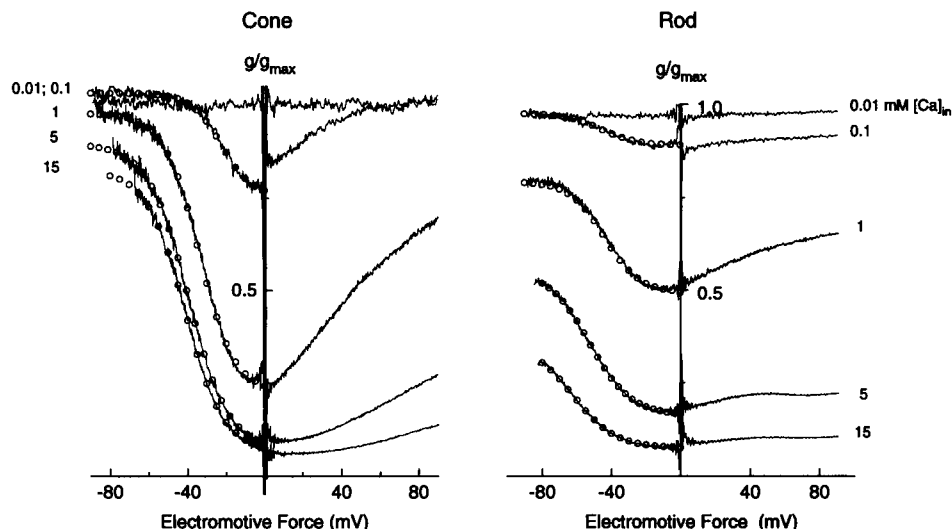
fore. Thus, the Ca^{2+}-blocking effect at its maximum is indistinguishable between receptor types; it has the same magnitude and nearly the same K_m and occurs at the zero current voltage. On the other hand, the extent of blockage changes with voltage. For example, at -70 mV emf, the K_m for Ca^{2+} block is 21.4 ± 4.8 mM ($n = 5$) in channels of cones, but it is 5.2 ± 0.7 mM ($n = 8$) in those of rods.

Although in rods a single site with asymmetric energy barriers seemed sufficient to explain some of the early Na^+ versus Ca^{2+} competition data (Zimmerman and Baylor, 1992), more recent experiments suggest that at least two blocking sites must be invoked to explain the effects of competition by other divalents (Karpen et al., 1993) and the current enhancement effects observed at low divalent concentrations (Tanaka and Furman, 1993). Recent experiments with structurally mutated bovine rod channels expressed in *Xenopus* oocytes provide convincing evidence for the existence of at least two sites. A structural mutation in glutamate 363 that prevents the blocking effect of extracellular Mg^{2+} fails to prevent the blocking effect of cytoplasmic Mg^{2+} and actually enhances it slightly (Root and McKinnon, 1993; Eisman et al., 1994). This suggests that E363 is a binding site for extracellular divalent cations and that a different site must exist for cytosolic cations. Also, Eisman et al. (1994) have found that the E363 mutation does

not affect the voltage-independent block. They suggest the existence of a cytosolic binding site for divalent cations that may control the probability of channel opening (rather than its open state conductance).

Our results strengthen the view that the cGMP-gated channels of both rods and cones have two binding sites for Ca^{2+}. One of the sites (site I) has the same energy of interaction with Ca^{2+} in both cell types and it is influenced to the same extent by the voltage field across the membrane. This conclusion is supported by the findings that (1) the maximal block by Ca^{2+} is indistinguishable between receptors in all its features, as discussed above, and (2) the Boltzmann function that describes the relief of Ca^{2+}-dependent block by hyperpolarizing voltages is nearly identical in the values of V_0 and κ in rods and cones. The second Ca^{2+}-binding site (site II) may be different. Either it has a higher energy of interaction with Ca^{2+} than the first one or it is located such that it is not influenced by the electric field across the membrane. Either mechanism makes it difficult to unblock channels by removing Ca^{2+} with voltage from the second site, at least over the voltage range we tested. As cones and rods differ in the fraction of channels unblocked by a given voltage, the simplest mechanism to explain the cone/rod differences would be to assume that the second site in cones has a weaker energy of interaction with Ca^{2+} or it

TABLE 1 cGMP-gated currents, voltage dependence of Ca^{2+} block, and adjustable parameters in Boltzmann function

[Ca²⁺] (mM)	Hyperpolarizing voltage								Depolarizing voltage		
	Cone				Rod				Cone		
	V_0 (mV)	κ (mV⁻¹)	max g/g_{max}*	min g/g_{max}†	V_0 (mV)	κ (mV⁻¹)	max g/g_{max}*	min g/g_{max}†	V_0 (mV)	κ (mV⁻¹)	max g/g_{max}*
0.1	-26.1 ± 5.3	-7.5 ± 0.6	0.99 ± 0.13	0.80 ± 0.06	-43.4 ± 2.1	$-7.9 + 3.2$	1.00 ± 0.03	0.92 ± 0.03	15.0 ± 0.6	19.0 ± 1.0	0.99 ± 0.09
1	-35.1 ± 2.4	$-10.0 + 1.5$	0.88 ± 0.15	0.33 ± 0.08	-41.0 ± 3.0	$-9.6 + 0.8$	0.79 ± 0.07	0.55 ± 0.07	33.1 ± 10.0	27.6 ± 5.0	0.74 ± 0.18
5	-43.6 ± 3.8	-11.8 ± 2.7	0.81 ± 0.14	0.18 ± 0.08	-49.9 ± 5.4	$-11.6 + 1.2$	0.56 ± 0.01	0.22 ± 0.06	61.6 ± 2.6	21.6 ± 4.8	0.38 ± 0.03
15	-48.8 ± 7.1	-11.7 ± 2.5	0.76 ± 0.18	0.15 ± 0.09	-57.2 ± 9.5	$-13.4 + 2.4$	0.43 ± 0.12	$0.13 + 0.06$	71.6 ± 2.3	12.6 ± 5.6	0.19 ± 0.03

The effects of depolarizing voltage on the current of rod channels could not be fit by the Boltzmann function.
*Maximum value of the normalized conductance.
†Minimum value of the normalized conductance.

is located such that it is more effectively influenced by voltage than the second site in rods. A weaker interaction of Ca^{2+} with the channel in cones logically leads to the expectation that Ca^{2+} transit is quicker in cones than in rods. Quicker transit would result in a larger fraction of the current being carried by Ca^{2+} than by Na and a higher Ca^{2+} permeability, relative to Na^+, in channels of cones than in those of rods, which is precisely what we have observed.

REFERENCES

Cobbs, W. H., and E. N. Pugh, Jr. 1987. Kinetics and components of the flash photocurrent of isolated retinal rods of the larval salamander, *Ambystoma tigrinum. J. Physiol.* 394:529–572.

Colamartino, G., A. Menini, and V. Torre. 1991. Blockage and permeation of divalent cations through the cyclic GMP-activated channels from tiger salamander retinal rods. *J. Physiol.* 440:189–206.

Eisman, E., F. Muller, S. H. Heinemann, and U. B. Kaupp. 1994. A single negative charge within the pore region of a cGMP-gated channel controls rectification, Ca blocking, and ionic selectivity. *Proc. Natl. Acad. Sci. USA.* 91:1109–1113.

Fain, G. L., and H. R. Matthews. 1990. Calcium and the mechanism of light adaptation in vertebrate photoreceptors. *Trends Neurosci.* 13:378–384.

Frings, S., R. Seifert, M. Godde, and U. B. Kaupp. Profoundly different calcium permeation and blockage determine the specific function of distinct cyclic nucleotide-gated channels. *Neuron.* In press.

Furman, R. E., and J. C. Tanaka. 1990. Monovalent selectivity of the cyclic guanosine monophosphate-activated ion channel. *J. Gen. Physiol.* 96:57–82.

Grey-Keller, M. P., and P. B. Detwiler. 1994. The calcium feedback signal in the phototransduction cascade of vertebrate rods. *Neuron.* 13:849–861.

Haynes, L. W. 1992. Block of the cyclic GMP-gated channel of vertebrate rod and cone photoreceptors by l-*cis*-diltiazem. *J. Gen. Physiol.* 100:783–801.

Haynes, L. W. 1993. Mono- and divalent cation selectivity of catfish cone outer segment cGMP-gated channels. *Biophys. J.* 64:A133.

Haynes, L. W., and K-W Yau. 1990. Single-channel measurements from the cGMP-activated conductance of catfish retinal cones. *J. Physiol.* 429:451–481.

Hestrin, S., and J. I. Korenbrot. 1990. Activation kinetics of retinal cones and rods: response to intense flashes of light. *J. Neurosci.* 10:1967–1973.

Hodgkin A. L., P. A. McNaugton, and B. J. Nunn. 1987. Measurement of sodium calcium exchange in salamander rods. *J. Physiol.* 391:347–370.

Karpen, J. W., R. L. Brown, L. Stryer, and D. A. Baylor. 1993. Interaction between divalent cations and the gating machinery of cyclic GMP-activated channels in salamander retinal rods. *J. Gen. Physiol.* 101:1–25.

Karpen, J. W., A. L. Zimmerman, L. Stryer, and D. A. Baylor. 1988. Molecular mechanics of the cyclic GMP-activated channel of retinal rods. *Cold Spring Harbor Symp. Quant. Biol.* 53:325–332.

Korenbrot, J. I., and D. L. Miller. 1986. Calcium ions act as modulators of intracellular information flow in retinal rod phototransduction. *Neuroscience Res.* 4:S11-S34.

Lagnado, L., L. Cervetto, and P. A. McNaughton. 1992. Calcium homeostasis in the outer segments of retinal rods from the tiger salamander. *J. Physiol.* 455:111–142.

Lewis, C. A. 1979. Ion-concentration dependence of the reversal potential and the single channel conductance of ion channels at the frog neuromuscular junction. *J. Physiol.* 286:417–445.

McNaughton, P. A. 1990. Light response of vertebrate photoreceptors. *Physiol. Rev.* 70:847–883.

Miller, D. L., and J. I. Korenbrot. 1987. Kinetics of light-dependent Ca fluxes across the plasma membrane of rod outer segments: a dynamic model of the regulation of cytoplasmic Ca concentration. *J. Gen. Physiol.* 90:397–426.

Miller, J. L., and J. I. Korenbrot. 1993a. In retinal cones, membrane depolarization in darkness activates the cGMP-dependent conductance: a model of Ca homeostasis and the regulation of guanylate cyclase. *J. Gen. Physiol.* 101:933–961.

Miller, J. L., and J. I. Korenbrot. 1993b. Phototransduction and adaptation in rods, single cones and twin cones of the striped bass retina: a comparative study. *Visual Neurosci.* 10:653–667.

Miller, J. L., and J. I. Korenbrot. 1994. Differences in Ca homeostasis between rod and cone photoreceptors revealed by the effects of voltage on the cGMP-conductance in intact cells. *J. Gen. Physiol.* 104:909–940.

Miller, J. L., A. Picones, and J. I. Korenbrot. 1994. Differences in transduction between rod and cone photoreceptors: an exploration of the role of calcium homeostasis. *Curr. Opin. Neurobiol.* 4:488–495.

Nakatani, K., and K.-W. Yau. 1988. Calcium and magnesium fluxes across the plasma membrane of the toad rod outer segment. *J. Physiol.* 395:695–729.

Perry, R J, and P. A. McNaughton. 1991. Response properties of cones from the retina of the tiger salamander. *J. Physiol.* 433:561–587.

Picones, A., and J. I. Korenbrot. 1992. Permeation and interaction of monovalent cations with the cGMP-gated channel of cone photoreceptors. *J. Gen. Physiol.* 100:647–673.

Picones A., and J. I. Korenbrot. 1995a. The PCa/PNa permeability ratio is higher in cGMP-gated channels of cone photoreceptors than in those of rods. *Biophys. J.* 68:A19

Picones, A., and J. I. Korenbrot. 1995b. Spontaneous, ligand-independent activity of the cGMP-gated ion channels in cone photoreceptors of fish. *J. Physiol.* 485:699–714.

Ratto, G. M., R. Payne, R. G. Owen, and R. Y. Tsien. 1988. The concentration of cytosolic free calcium in vertebrate rod outer segment measured with Fura-2. *J. Neurosci.* 8:3240–3246.

Root, M. J., and R. MacKinnon. 1993. Identification of an external divalent cation-binding site in the pore of a cGMP-activated channel. *Neuron.* 11:459–466.

Tanaka, J. C. 1993. The effects of protons on 3',5'-cGMP-activated currents in photoreceptor patches. *Biophys. J.* 65:2517–2523.

Tanaka, J. C., and R. E. Furman. 1993. Divalent effects on cGMP-activated currents in excised patches from amphibian photoreceptors. *J. Membr. Biol.* 131:245–256.

Tomura, T., K. Nakatani, and Yau K.-W. 1991. Calcium feedback and sensitivity regulation in primate rods. *J. Gen. Physiol.* 98:95–130.

Torre, V., H. R. Matthews, and T. D. Lamb. 1986. The role of calcium in regulating the cyclic GMP cascade of phototransduction in retinal rods. *Proc. Natl. Acad. Sci. USA.* 83:7109–7113.

Yau, K.-W., and D. A. Baylor. 1989. Cyclic GMP-activated conductance of retinal photoreceptor cells. *Annu. Rev. Neurosci.* 12:289–327.

Yau, K.-W., and K. Nakatani. 1985. Light-induced reduction of cytoplasmic free calcium in retinal rod outer segment. *Nature.* 313:579–582.

Zimmerman, A. L., and D. A. Baylor. 1992. Cation interaction within the cyclic-GMP-activated channel of retinal rods from the tiger salamander. *J. Physiol.* 449:759–783.